

The location of potential energy sources and the export of dense water from the Atlantic Ocean

K. I. C. Oliver^{1,2}, N. R. Edwards¹

Kevin Oliver, Department of Earth and Environmental Sciences, The Open University, Walton Hall, Milton Keynes, MK7 6AA, U.K. (k.i.c.oliver@open.ac.uk).

¹Department of Earth and Environmental Sciences, CEPSAR, The Open University, Milton Keynes, UK

²Department of Earth Sciences, University of Oxford, UK

The export of dense water from the Atlantic and into the Indo-Pacific oceans, and heat transport in the opposite direction, is traditionally attributed to the fact that dense water forms in the Atlantic but not the Pacific. Evidence from two models, presented here, suggests this is an incomplete explanation. It is found that dense water export from the Atlantic depends on a potential energy (PE) sink, associated with dense water downwelling in the Atlantic, that is not balanced by a PE source within the Atlantic. Therefore, increasing the Atlantic PE source reduces dense Atlantic water export. Tide models suggest that the Atlantic PE source may have been much higher at the last glacial maximum. This could have significantly reduced dense water export from the Atlantic Ocean, even if Atlantic overturning was stronger than it is today.

1. Introduction

A major feature of global ocean circulation is the asymmetry in overturning between the Atlantic and Indo-Pacific oceans. There is net export of dense water from the Atlantic Ocean and an import of dense water into the Indo-Pacific. Whereas the principal upwelling region for exported Atlantic water is the Antarctic Circumpolar Current (ACC), and the Southern Ocean is also the major source region for deep water in the Indo-Pacific, the sum of these cells is a net transport of dense water from the Atlantic to the Indo-Pacific basins, associated with ocean heat transport in the opposite direction and equatorward heat transport in the South Atlantic (Ganachaud and Wunsch, 2000). This circulation is attributed to the fact that dense water forms in the Atlantic but not the Pacific (Broecker, 1987). In this study, we present evidence that this interpretation is incomplete.

The global meridional overturning circulation (MOC) consumes gravitational potential energy (PE) by the downwelling of dense water at high latitudes and upwelling of lighter water elsewhere. A prevailing paradigm is that the rate at which this PE is replenished controls the strength of the global MOC at equilibrium, although the identity of the key PE sources remains controversial (Munk and Wunsch, 1998; Webb and Suginohara, 2001; Tailleux, 2008). PE generation is equivalent to the downwelling of buoyancy, either by diapycnal mixing or by wind-driven upwelling of dense water (and associated downwelling of light water), and therefore PE sources are essential to set up vertical shear in horizontal pressure gradients which drive the thermohaline (THC) component of the MOC (Oliver *et al.*, 2005). Since theory predicts that the basin-scale flow in the THC is down pressure gradients (Bryan, 1987), this implies that overturning in the ocean is sensitive to the

distribution of PE sources as well as their magnitude. It is likely that there is a greater diabatic PE source in the Indo-Pacific oceans than the smaller Atlantic Ocean, leading to the hypothesis that the relative lack of PE generation in the Atlantic Ocean is a key cause of net export of dense water from the Atlantic. Here, we vary the distribution of PE sources and sinks in a two-dimensional (2D) ocean model and a three-dimensional (3D) climate model, in order to test this hypothesis.

2. Experiments with a two-dimensional ocean model

2.1. Experiment design

Experiments were conducted with a 2D ocean model with a horizontal resolution of 5° , and consisting of two basins (representing the Atlantic and Indo-Pacific oceans) which connect at 30°S to form the Southern Ocean. The Indo-Pacific basin is three times the width of the Atlantic basin at all latitudes. The bathymetric depth is 5 km. We use density as the vertical coordinate to remove diapycnal leakage and enable accurate diagnosis of the PE budget. There are 14 layers. With the linear equation of state applied here, buoyancy conservation implies for the ocean interior:

$$(\eta_\rho)_t = -(v\eta_\rho)_I + (\kappa_A(\eta_\rho)_I)_I - (\kappa_v\rho_z)_{\rho\rho}, \quad (1)$$

where $\eta_\rho = \rho_z^{-1}$ is the inverse of vertical density stratification (and may be discretised as $h/\delta\rho$ where h is layer thickness and $\delta\rho$ is the vertical resolution), v is meridional velocity, and κ_A and κ_v are isopycnal and diapycnal diffusivities respectively. The t , I and ρ subscripts denote differentiation with respect to time, latitude (but along an isopycnal surface), and the vertical density coordinate, respectively. The central assumption of 2D models is that meridional pressure gradients drive meridional flow (Wright and Stocker,

1991; Mohammad and Nilsson, 2006):

$$\gamma v_p = -\rho_0^{-1} p_y \quad (2)$$

where v_p is the pressure gradient–driven flow, p_y is the meridional pressure gradient, ρ_0 is the reference density, and γ is an input coefficient which implicitly relates meridional gradients to zonal gradients. An exception to (2) applied in this study is the region 50 to 60°S between the surface and 2000 m depth, representing the zonally periodic ACC where there is no mean pressure gradient–driven meridional flow. Here, meridional gradients can only be removed by isopycnal diffusion (which parameterises eddy fluxes): κ_A is horizontally uniform and decreases from 4000 m² s⁻¹ at the surface to 400 m² s⁻¹ at depths greater than 2000 m (c.f. Danabasoglu and Marshall, 2007). The remaining governing equations are hydrostatic equilibrium and continuity: $p_z = -g\rho$ and $v_y + w_z = 0$, respectively, where w is vertical velocity and subscripts denote differentiation. There is no flow through horizontal or vertical boundaries. Surface densities are held fixed at zonally averaged climatological winter densities (Levitus and Boyer, 1994). Zonally and annually averaged surface wind stresses (Josey *et al.*, 1998) are also applied.

The local PE source due to diapycnal mixing, $g\kappa_v(-\rho_z)\rho_0^{-1}$, is set temporally constant, resulting in a stratification–dependent diapycnal diffusivity:

$$\kappa_v(y, z) = \kappa_c(y, z) \frac{\rho_{z0}(z)}{\rho_z(y, z)}, \quad \kappa_c(y, z) = \kappa_0 + \kappa_{dp}(y) e^{(z_{dp}-z)/z_{sc}}, \quad (3)$$

where ρ_{z0} is the fit of an exponential function to a global mean vertical density gradient profile (Levitus and Boyer, 1994), $\rho_{z0} = -5.5e^{z/z_l} \times 10^{-3}$ kg m⁻⁴, where $z_l = 650$ m. To derive κ_c , we use here $\kappa_0 = 0.1$ cm² s⁻¹, $z_{dp} = -2500$ m, $z_{sc} = 800$ m, and $\kappa_{dp} = 1$ cm² s⁻¹ in the control experiment at all locations. This horizontally uniform PE source results

in a three times greater PE source in the Indo-Pacific than in the Atlantic. In “High Atlantic PE” experiments, κ_{dp} is increased to $5 \text{ cm}^2 \text{ s}^{-1}$ in the North Atlantic, which increases the PE source in the Atlantic to approximately equal that in the Indo-Pacific. The increased PE source in the Atlantic is weighted towards the deep North Atlantic in this way because tide model studies suggest that tidal energy dissipation in the deep North Atlantic is particularly sensitive to changes in sea level (Thomas and Sündermann, 1999; Egbert *et al.*, 2004). A further cause of asymmetry in the model is removed in “Dense Pacific” experiments by replacing the Indo-Pacific surface density field with the equivalent field from the Atlantic Ocean. We thus determine the relative importance of the asymmetry in dense water formation and the asymmetry in PE sources, in controlling the net dense outflow from the Atlantic to the Indo-Pacific oceans.

2.2. Control Experiment

Fig 1a shows the equilibrium density field and circulation in the control run. The maximum in the Atlantic overturning streamfunction ψ^A is 16 Sv, of which 7 Sv of dense water is exported to be upwelled either in the ACC or the Indo-Pacific Ocean. Additionally, there is formation of Antarctic bottom water ($\psi^S = -29$ Sv; anticlockwise cells are negative by convention), and a -3 Sv Antarctic cell in the Atlantic Ocean. Because North Pacific water is much lighter than Antarctic and Atlantic surface waters, the maximum in Indo-Pacific overturning is shallow and weak ($\psi^P = 2$ Sv). Instead, there is an overturning cell of -16 Sv in the Indo-Pacific, consisting of water of both Atlantic and Antarctic origin. The net export of dense water from the Atlantic to the Indo-Pacific $\psi^{A \rightarrow P}$ is defined as

the mean of the export of water with $\sigma_0 \geq 27.61$ from the Atlantic and the import of water of this density class to the Indo-Pacific, yielding $\psi^{A \rightarrow P} = 11$ Sv.

Global overturning is an adiabatic net PE sink, due to the downwelling of dense water and upwelling of lighter water. This is the sum of pressure gradient–driven, wind–driven, and isopycnal mixing terms. Integrated globally, wind provides a PE source of 1.7 TW and isopycnal mixing is a PE sink of 1.7 TW in the control simulation, both dominated by the ACC and the region immediately to its north. Pressure gradient–driven flow is a PE sink of 1.4 TW, yielding a total adiabatic PE sink of 1.4 TW, balanced at equilibrium by the diabatic PE source due to diapycnal mixing. The overturning circulation may be understood in terms of the distribution of these PE sources and sinks. The 0.8 TW provided by Indo-Pacific diapycnal mixing is three times greater than the Atlantic PE source, owing to the basins’ relative sizes. However, the vigorous Atlantic overturning cell consumes seven times more energy (0.7 TW) than Pacific overturning, owing to the greater density of North Atlantic waters. As a result, Atlantic overturning consumes PE that is generated outside the Atlantic Ocean. This is only possible if the Atlantic cell is not confined within the Atlantic, since the PE budget must balance locally at steady state. Therefore, there is dense water export from the Atlantic Ocean. Similarly, PE generation in the Indo-Pacific basin helps to sustain Antarctic and Atlantic overturning because it exceeds the PE consumption in Pacific overturning.

The ocean adjusts to this equilibrium between PE sources and sinks by the mechanism of pressure gradient–driven flow. The PE source in the Indo-Pacific equates to a downwelling of buoyancy. Lighter deep waters in the Indo-Pacific than the Atlantic Ocean (Fig 1a)

lead to greater upper ocean pressures in the Indo-Pacific than the Atlantic, and greater deep ocean pressures in the Atlantic than the Pacific. In a 2D framework, this drives a net flow of dense water from the Atlantic to the Pacific Ocean, leading to an upwelling of buoyancy in the Pacific which locally balances buoyancy downwelling due to diapycnal mixing.

2.3. The role of asymmetries in surface density and PE sources

We now consider the relative importance of the two major asymmetries in the global PE budget: greater PE consumption in Atlantic overturning than Pacific overturning, and greater PE generation in the Indo-Pacific than the Atlantic. Fig 1c shows the results of a “Dense Pacific” experiment with identical Atlantic and Indo-Pacific surface densities. Dense water formation in the North Pacific results in a 30 Sv Pacific overturning cell, whereas ψ^A decreases slightly to 14 Sv. $\psi^{A \rightarrow P}$ also decreases, but remains positive (5 Sv) despite much stronger overturning in the Indo-Pacific than the Atlantic. This is associated with the larger PE source in the Indo-Pacific than the Atlantic. PE consumption due to Pacific overturning (0.4 TW) remains smaller than the PE supply in the Indo-Pacific oceans (0.8 TW), whereas PE consumption due to Atlantic overturning (0.4 TW) remains greater than the PE supply in the Atlantic Ocean (0.3 TW).

Fig 1b shows the results of a “High Atlantic PE” experiment in which the Atlantic diabatic PE source is increased to 0.8 TW, approximately equal to the Indo-Pacific diabatic PE source (see Section 2.1). The additional North Atlantic PE source deepens isopycnals in the deep Atlantic Ocean, increasing meridional pressure gradients between the low and high latitude North Atlantic, and causing ψ^A to increase to 30 Sv. However, the deepening

of isopycnals also reverses the sign of meridional pressure gradients in much of the South Atlantic Ocean, so that the Antarctic cell expands at the expense of the Atlantic cell, and much of the additional PE source is consumed in the Antarctic cell rather than the Atlantic cell. PE consumption in the Atlantic cell increases by 0.2 TW, compared with a 0.5 TW increase in the Atlantic PE source. Therefore, there is sufficient PE generation within the Atlantic Ocean to sustain Atlantic overturning, although some of this energy is used to sustain a -6 Sv Antarctic cell within the Atlantic. The result of this is that the net export from the Atlantic to the Pacific, $\psi^{A \rightarrow P}$, decreases to 6 Sv. A “High Atlantic PE + Dense Pacific” experiment is presented in Fig 1d. We obtain the maxima in overturning: $\psi^P = 32$ Sv, $\psi^A = 29$ Sv and $\psi^S = -28$ Sv. The asymmetry in overturning between the Atlantic and the Indo-Pacific is almost removed ($\psi^{A \rightarrow P} = -0.3$ Sv).

Finally, the total Atlantic diabatic PE source was varied between 0.1 and 1.1 TW in a series of experiments by varying κ_{dp} between 0 and $8 \text{ cm}^2 \text{ s}^{-1}$ in the North Atlantic only. Atlantic overturning strength increases by 25 Sv across this parameter range (Fig 2a) as the PE source increases, but $\psi^{A \rightarrow P}$ decreases from 12 to 4 Sv in experiments with surface density fields identical to the control experiment, and from 7 Sv to -4 Sv in “Dense Pacific” experiments (Fig 2b). We also consider the effect of these changes on global overturning, which we define as $\psi^A + \psi^P - \psi^S$. In both sets of experiments, the dependence of global overturning on the global mean diffusivity closely follows the $\frac{2}{3}$ power law from MOC theory (Bryan, 1987) despite the complication of wind-driven circulation (Fig 2c); the relationship between overturning and the global PE source also follows this power law, though less precisely (Fig 2d). However, we obtain stronger global overturning,

given the same global PE source, in the “Dense Pacific” experiments as opposed to the “Levitus surface density” experiments.

3. Experiments with a three-dimensional coupled climate model

To this point we have assumed a linear relationship between meridional pressure gradients and meridional flow, and neglected climate feedbacks by imposing a fixed surface density field. It is therefore useful to test whether our findings are robust to the application of 3D dynamics, complex topography, and to atmospheric and cryospheric feedbacks. Therefore, the control and “High Atlantic PE” experiments were repeated in the coupled model of Edwards and Marsh [2005], implemented in the GENIE framework (“Dense Pacific” experiments were not repeated because surface densities are free to vary in the coupled model). The ocean is z -coordinate, frictional-geostrophic, has 36×36 surface grid points, and is coupled to an atmospheric energy and moisture balance model and a dynamic sea-ice module. We use the parameters of GENIE-1 defined by Hargreaves *et al.* [2004], except that uniform diffusivity is replaced by the relationship defined in (3) and the number of vertical levels is doubled to 16.

Fig 2 shows the relationship between PE sources and overturning as κ_{dp} in the North Atlantic basin is increased from 0 to $10 \text{ cm}^2 \text{ s}^{-1}$. The dependence of global overturning on the global diabatic PE source is slightly stronger than that given by a $\frac{2}{3}$ power law. There is no clear relationship between mean diffusivity and global overturning (Fig 2c) because of very high diffusivities in a small number of weakly stratified cells. If these grid-points are downweighted by taking logs before averaging, the relationship is similar to that obtained in the 2D model (Fig 2e). The increase in Atlantic overturning caused

by the additional PE supply in North Atlantic basin is only 8 Sv across the domain of κ_{dp} (Fig 2a). Nevertheless, the decrease in net export of dense water from the Atlantic to the Indo-Pacific basin is similar to that obtained in the 2D model (Fig 2b), providing further support to the hypothesis that an important driver of dense water export from the Atlantic to the Indo-Pacific is the asymmetry in the magnitude of the PE sources. Density and overturning streamfunction sections for the control simulation ($\kappa_{dp} = 1 \text{ cm}^2 \text{ s}^{-1}$) and a high Atlantic PE simulation ($\kappa_{dp} = 5 \text{ cm}^2 \text{ s}^{-1}$ in the North Atlantic) are included as auxiliary materials.

4. Discussion

We have found that the strength of dense water export from the Atlantic depends both on the relative strength of overturning in the Atlantic and the Pacific, and on the distribution of PE sources in the ocean. Thus, in a 2D model, a substantial (albeit reduced) dense water export from the Atlantic is maintained even if the Pacific overturning transport is increased from near zero to more than double the Atlantic overturning transport. Moreover, in both a 2D ocean model and a 3D climate model, the net export of dense water from the Atlantic to the Indo-Pacific oceans is sensitive to the distribution of PE sources. Atlantic dense water export may be reduced by increasing the PE source in the Atlantic, despite a resulting increase in Atlantic overturning.

Today, the Indo-Pacific oceans probably provide a much greater diabatic PE source than the Atlantic due to their greater size. At the last glacial maximum (LGM), however, tide model evidence suggests tidal energy dissipation rates below 1000 m in the North Atlantic Ocean that were an order of magnitude greater than in the present day (Egbert *et al.*, 2004;

their Figure 10). Barring a change in the relationship between kinetic energy dissipation and PE production, this would have led to a large increase in the Atlantic PE source. Additionally, sediment pore waters indicate that the density difference between Antarctic and Atlantic source waters was probably significantly greater at the LGM (Adkins *et al.*, 2002). We speculate, with the support of idealised simulations with the 2D model, that this redistribution of PE sources and sinks would favour a shallow Atlantic overturning cell with reduced export from the Atlantic basin. Figs 1e,f show the results of repetitions of control and “High Atlantic PE” experiments of (Figs 1a,b), but where the surface density in the southernmost grid cell is increased by 0.6 kg m^{-3} to obtain Antarctic waters that are 0.9 kg m^{-3} denser than Atlantic waters, consistent with Adkins *et al.* [2002]. In Fig 1e, this results in an increased and expanded Antarctic overturning cell, which is associated with a shallow and weak (9 Sv) Atlantic cell. However, in the presence of an increased Atlantic PE source, the Atlantic overturning is reasonably strong (16 Sv), despite remaining shallow, and the export of Atlantic water is further reduced to 2 Sv (Fig 1f). This is consistent with interpretations of several paleo-data sources as suggesting a contraction of the Atlantic cell and a reduction/reversal of Atlantic water export from the Atlantic Ocean (Marchitto and Broecker, 2006; Curry and Oppo, 2005; Lynch-Stieglitz *et al.*, 2006), despite the persistence of Atlantic overturning at the LGM. The eventual test for the plausibility of a dramatically increased North Atlantic PE source at the LGM will be the comparison of model results, including such paleoceanographic proxies, with the LGM sediment record.

Acknowledgments. K. Oliver was supported by a Leverhulme Trust Early Career Fellowship, and this study was further supported by NERC Quaternary QUEST.

References

- Adkins, J. F., McIntyre, K., and Schrag, D. P. (2002). The salinity, temperature and delta O-18 of the glacial deep ocean. *Science*, **298**, 1769–1773.
- Broecker, W. S. (1987). Unpleasant surprises in the greenhouse? *Nature*, **328**, 123–126.
- Bryan, F. (1987). Parameter sensitivity of primitive equation ocean general circulation models. *J. Phys. Oceanogr.*, **17**, 970–985.
- Curry, W. B. and Oppo, D. W. (2005). Glacial water mass geometry and the distribution of delta-13C of Sigma-CO2 in the western Atlantic Ocean. *Paleoceanogr.*, **20**, PA1017, doi:10.1029/2004PA001021.
- Danabasoglu, G. and Marshall, J. (2007). Effects of vertical variations of thickness diffusivity in an ocean general circulation model. *Ocean Model.*, **18**, 122–141.
- Edwards, N. R. and Marsh, R. (2005). Uncertainties due to transport-parameter sensitivity in an efficient 3-d ocean-climate model. *Clim. Dyn.*, **24**, 415–433.
- Egbert, G. D., Ray, R. D., and Bills, B. G. (2004). Numerical modeling of the global semidiurnal tide in the present day and in the last glacial maximum. *J. Geophys. Res.*, **109**, 10.1029/2003JC001973.
- Ganachaud, A. S. and Wunsch, C. (2000). Improved estimates of global ocean circulation, heat transport and mixing from hydrographic data. *Nature*, **408**, 453–457.
- Hargreaves, J. C., Annan, J. D., Edwards, N. R., and Marsh, R. (2004). An efficient climate forecasting method using an intermediate complexity Earth System Model and

the ensemble Kalman filter. *Clim. Dyn.*, **23**, 745–760.

Josey, S. A., Kent, E. C., and Taylor, P. K. (1998). *The Southampton Oceanography Centre (SOC) Ocean-Atmosphere Heat, Momentum and Freshwater Flux Atlas*. Southampton Oceanography Centre Report 6, 30pp + plates.

Levitus, S. and Boyer, T. (1994). World ocean atlas 1994 volume 4: Temperature. *NOAA Atlas NESDIS 4*, U.S. Department of Commerce, Washington, D.C., **59**, 75–176.

Lynch-Stieglitz, J., Curry, W., and Oppo, D. (2006). Meridional overturning circulation in the South Atlantic at the last glacial maximum. *Geochem. Geophys. Geosyst.*, **7**, doi:10.1029/2005GC001226.

Marchitto, T. M. and Broecker, W. S. (2006). Deep water mass geometry in the glacial Atlantic Ocean: A review of constraints from the paleonutrient proxy Cd/Ca. *Geochem. Geophys. Geosyst.*, **7**, 10.1029/2006GC001323.

Mohammad, R. and Nilsson, J. (2006). Symmetric and asymmetric modes of the thermohaline circulation. *Tellus*, **58A**, 616–627.

Munk, W. and Wunsch, C. (1998). Abyssal recipes II: Energetics of tidal and wind mixing. *Deep-Sea Res. I*, **45**, 1977–2010.

Oliver, K. I. C., Watson, A. J., and Stevens, D. P. (2005). Can limited ocean mixing buffer rapid climate change? *Tellus*, **57A**, 676–690.

Tailleux, R. (2008). On the energetics of stratified turbulent mixing, irreversible thermodynamics, Boussinesq models, and the ocean heat engine controversy. submitted to *J. Fluid Mech.*

- Thomas, M. and Sündermann, J. (1999). Tides and torques of the world ocean since the last glacial maximum. *J. Geophys. Res.*, **104**(C2), 3159–3183.
- Webb, D. J. and Sugimotohara, N. (2001). Vertical mixing in the ocean. *Nature*, **409**, 37.
- Wright, D. G. and Stocker, T. F. (1991). A zonally averaged ocean model for the thermohaline circulation, Part I: Model development and flow dynamics. *J. Phys. Oceanogr.*, **21**, 1713–1724.

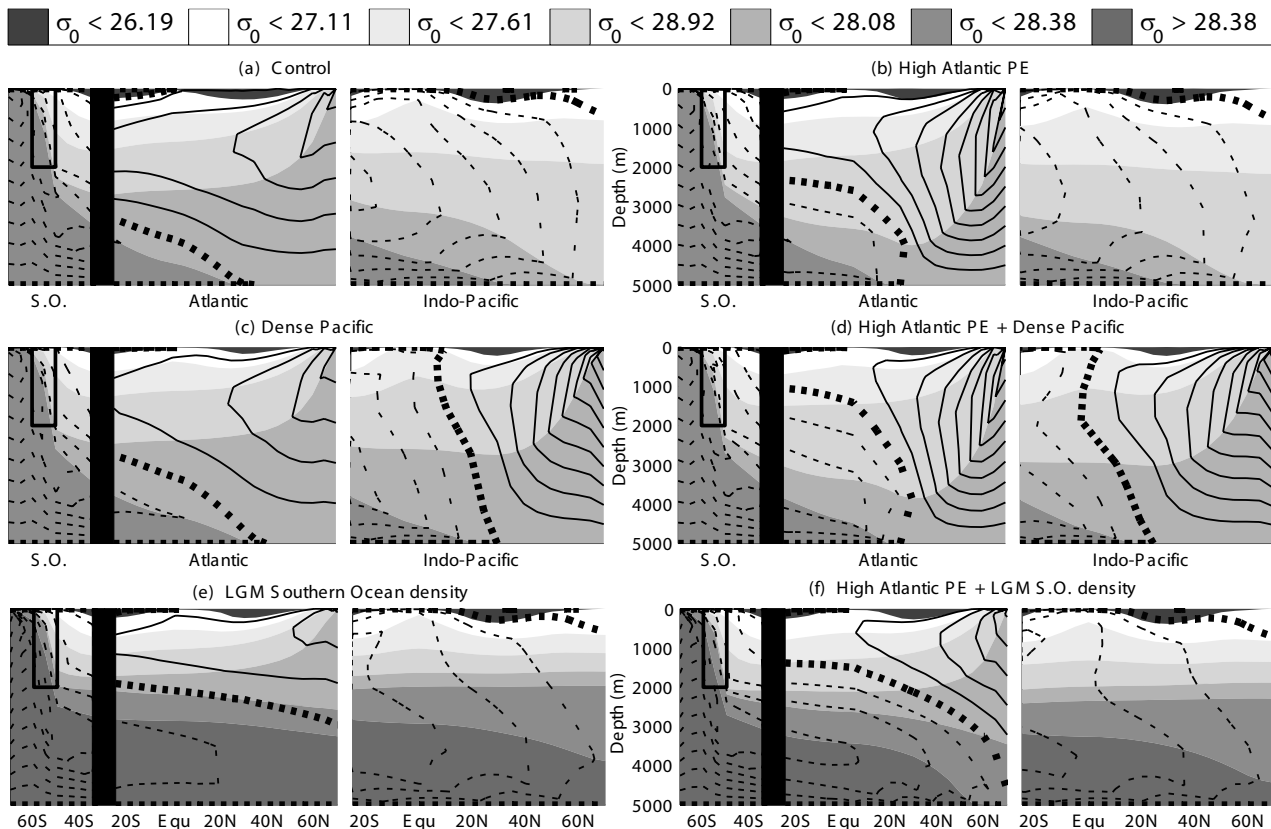


Figure 1. Equilibrium density (shading) and overturning streamfunction (contours) sections in the 2D model for: (a) the control simulation; (b) a simulation with κ_{dp} increased to $5 \text{ cm}^2 \text{ s}^{-1}$ in the North Atlantic Ocean; (c) and (d) are equivalent to (a) and (b), respectively, but with Indo-Pacific surface densities set equal to Atlantic surface densities; (e) and (f) are equivalent to (a) and (b), respectively, but with surface density in the southernmost grid cell increased by 0.6 kg m^{-3} to represent likely conditions at the last glacial maximum (LGM; see Section 4). Solid contours are positive (clockwise), dashed are negative, and bold dashed is 0 Sv , with an interval of 3 Sv . S.O. \equiv Southern Ocean. The 2000 m deep box in the Southern Ocean is the region where there is no pressure gradient–driven meridional flow.

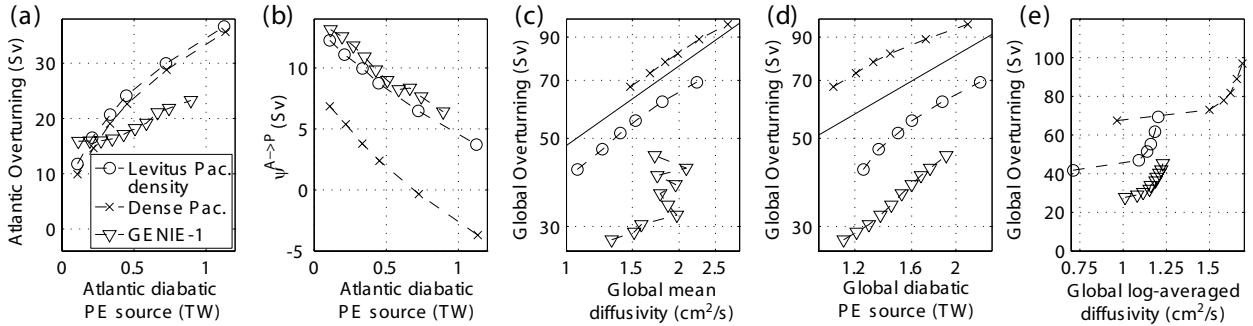


Figure 2. The effect on overturning of varying κ_{dp} between 0 and $8 \text{ cm}^2 \text{ s}^{-1}$ in the North Atlantic: (a) ψ^A and (b) $\psi^{A \rightarrow P}$ plotted against the Atlantic diabatic PE source. Global overturning is plotted against (c) global mean vertical diffusivity; (d) the global diabatic PE source; and (e) log-averaged diffusivity $= e^{\overline{\ln(\kappa_v)}}$. The solid line in (c) and (d) shows the gradient associated with the equation $y = y_0 x^{2/3}$ in log-log space. “GENIE-1” experiments were carried out using the climate model (Section 3); other experiments were carried out using the ocean model (Section 2), either with the same surface density field as the control experiment (“Levitus Pac. density”), or with surface densities in the Indo-Pacific increased to match those in the Atlantic (“Dense Pac.”).